ELSEVIER

Chemical Engineering and Processing 41 (2002) 551–561

Chemical Engineering and Processing

www.elsevier.com/locate/cep

Evaluation of steam jet ejectors

Hisham El-Dessouky *, Hisham Ettouney, Imad Alatiqi, Ghada Al-Nuwaibit

Department of Chemical Engineering, College of Engineering and Petroleum, Kuwait University, P.O. Box 5969, Safat 13060, Kuwait

Received 4 April 2001; received in revised form 26 September 2001; accepted 27 September 2001

Abstract

Steam jet ejectors are an essential part in refrigeration and air conditioning, desalination, petroleum refining, petrochemical and chemical industries. The ejectors form an integral part of distillation columns, condensers and other heat exchange processes. In this study, semi-empirical models are developed for design and rating of steam jet ejectors. The model gives the entrainment ratio as a function of the expansion ratio and the pressures of the entrained vapor, motive steam and compressed vapor. Also, correlations are developed for the motive steam pressure at the nozzle exit as a function of the evaporator and condenser pressures and the area ratios as a function of the entrainment ratio and the stream pressures. This allows for full design of the ejector, where defining the ejector load and the pressures of the motive steam, evaporator and condenser gives the entrainment ratio, the motive steam pressure at the nozzle outlet and the cross section areas of the diffuser and the nozzle. The developed correlations are based on large database that includes manufacturer design data and experimental data. The model includes correlations for the choked flow with compression ratios above 1.8. In addition, a correlation is provided for the non-choked flow with compression ratios below 1.8. The values of the coefficient of determination (R^2) are 0.85 and 0.78 for the choked and non-choked flow correlations, respectively. As for the correlations for the motive steam pressure at the nozzle outlet and the area ratios, all have R^2 values above 0.99.

Keywords: Steam jet ejectors; Choked flow; Heat pumps; Thermal vapor compression

1. Introduction

Currently, most of the conventional cooling and refrigeration systems are based on mechanical vapor compression (MVC). These cycles are powered by a high quality form of energy, electrical energy. The inefficient use of the energy required to operate such a process can be generated by the combustion of fossil fuels and thus contributes to an increase in greenhouse gases and the generation of air pollutants, such as NOx, SOx, particulates and ozone. These pollutants have adverse effects on human health and the environment. In addition, MVC refrigeration and cooling cycles use unfriendly chloro-floro-carbon compounds (CFCs), which, upon release, contributes to the destruction of the protective ozone layer in the upper atmosphere. Environmental considerations and the need for efficient use of available energy call for the development of processes based on the use of low grade heat. These processes adopt entrainment and compression of low pressure vapor to higher pressures suitable for different systems. The compression process takes place in absorption, adsorption, chemical or jet ejector vapor compression cycles. Jet ejectors have the simplest configuration among various vapor compression cycles. In contrast to other processes, ejectors are formed of a single unit connected to tubing of motive, entrained and mixture streams. Also, ejectors do not include valves, rotors or other moving parts and are available commercially in various sizes and for different applications. Jet ejectors have lower capital and maintenance cost than the other configurations. On the other hand, the main drawbacks of jet ejectors include the following:

- Ejectors are designed to operate at a single optimum point. Deviation from this optimum results in dramatic deterioration of the ejector performance.

* Corresponding author. Tel.: +965-4811188x5613; fax: +965-4839498.

E-mail address: eldessouky@kuc01.kuniv.edu.kw (H. El-Dessouky).

0255-2701/02/$ - see front matter
PII: S0255-2701(01)00176-3

- Ejectors have very low thermal efficiency.

Applications of jet ejectors include refrigeration, air conditioning, removal of non-condensable gases, transport of solids and gas recovery. The function of the jet ejector differs considerably in these processes. For example, in refrigeration and air conditioning cycles, the ejector compresses the entrained vapor to higher pressure, which allows for condensation at a higher temperature. Also, the ejector entrainment process sustains the low pressure on the evaporator side, which allows evaporation at low temperature. As a result, the cold evaporator fluid can be used for refrigeration and cooling functions. As for the removal of non-condensable gases in heat transfer units, the ejector entrainment process prevents their accumulation within condensers or evaporators. The presence of non-condensable gases in heat exchange units reduces the heat transfer efficiency and increases the condensation temperature because of their low thermal conductivity. Also, the presence of these gases enhances corrosion reactions. However, the ejector cycle for cooling and refrigeration has lower efficiency than the MVC units, but their merits are manifested upon the use of low grade energy that has limited effect on the environment and lower cooling and heating unit cost.

Although the construction and operation principles of jet ejectors are well known, the following sections provide a brief summary of the major features of ejectors. This is necessary in order to follow the discussion and analysis that follow. The conventional steam jet ejector has three main parts: (1) the nozzle; (2) the suction chamber; and (3) the diffuser (Fig. 1). The nozzle and the diffuser have the geometry of converging/diverging venturi. The diameters and lengths of various parts forming the nozzle, the diffuser and the suction chamber, together with the stream flow rate and properties, define the ejector capacity and performance. The ejector capacity is defined in terms of the flow rates of the motive steam and the entrained vapor. The sum of the motive and entrained vapor mass flow rates gives the mass flow rate of the compressed vapor. As for the ejector performance, it is defined in terms of entrainment, expansion and compression ratios. The entrainment ratio (w) is the flow rate of the entrained vapor

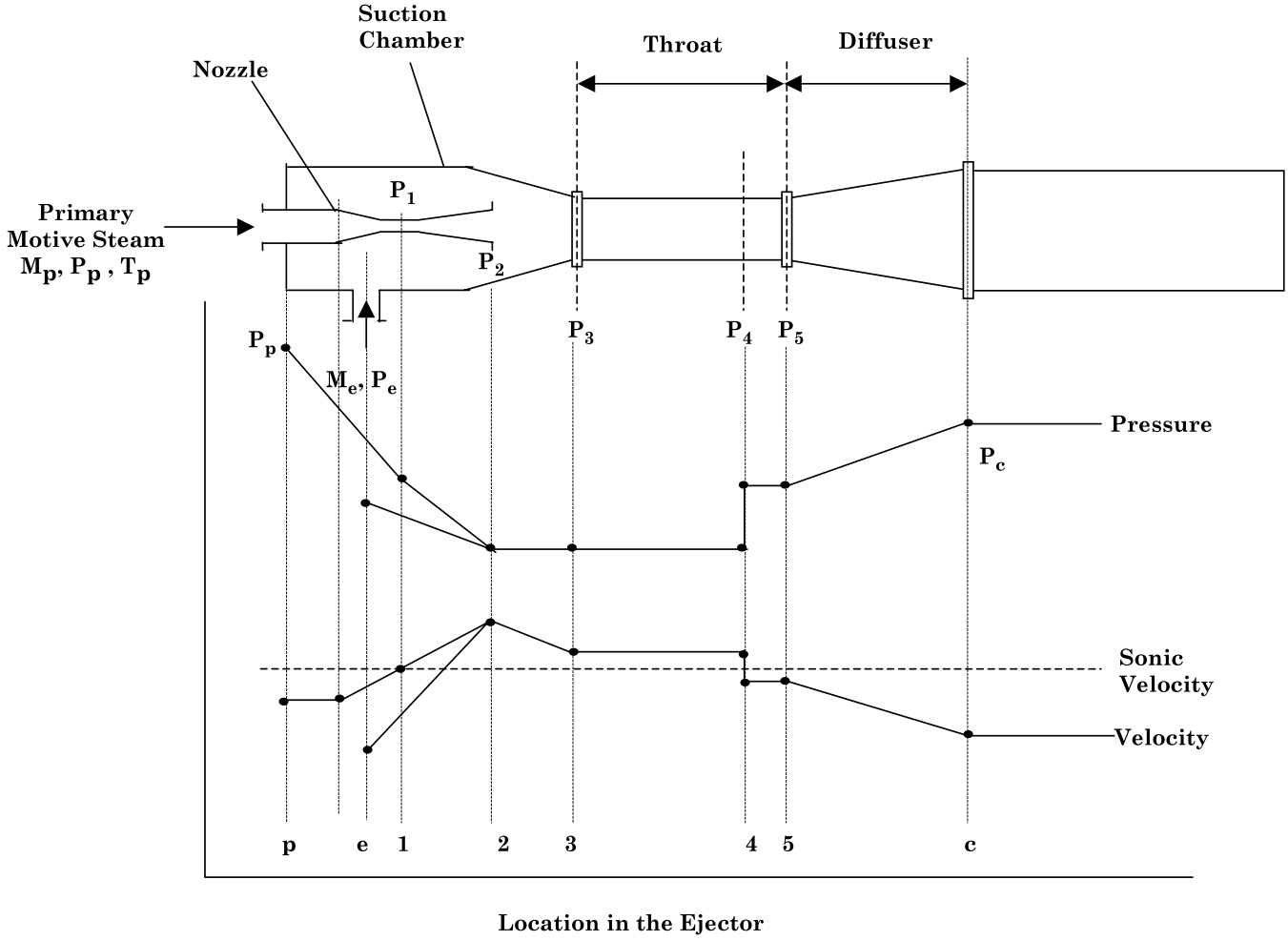

Fig. 1. Variation in stream pressure and velocity as a function of location along the ejector.

divided by the flow rate of the motive steam. As for the expansion ratio (Er), it is defined as the ratio of the motive steam pressure to the entrained vapor pressure. The compression ratio (Cr) gives the pressure ratio of the compressed vapor to the entrained vapor.

Variations in the stream velocity and pressure as a function of location inside the ejector, which are shown in Fig. 1, are explained below:

- The motive steam enters the ejector at point (p) with a subsonic velocity.
- As the stream flows in the converging part of the ejector, its pressure is reduced and its velocity increases. The stream reaches sonic velocity at the nozzle throat, where its Mach number is equal to one.
- The increase in the cross section area in the diverging part of the nozzle results in a decrease of the shock wave pressure and an increase in its velocity to supersonic conditions.
- At the nozzle outlet plane, point (2), the motive steam pressure becomes lower than the entrained vapor pressure and its velocity ranges between 900 and 1200 m/s.
- The entrained vapor at point (e) enters the ejector, where its velocity increases and its pressure decreases to that of point (3).
- The motive steam and entrained vapor streams may mix within the suction chamber and the converging section of the diffuser or it may flow as two separate streams as it enters the constant cross section area of the diffuser, where mixing occurs.
- In either case, the mixture goes through a shock inside the constant cross section area of the diffuser. The shock is associated with an increase in the mixture pressure and reduction of the mixture velocity to subsonic conditions, point (4). The shock occurs because of the back pressure resistance of the condenser.
- As the subsonic mixture emerges from the constant cross section area of the diffuser, further pressure increase occurs in the diverging section of the diffuser, where part of the kinetic energy of the mixture is converted into pressure. The pressure of the emerging fluid is slightly higher than the condenser pressure, point (c).

Summary for a number of literature studies on ejector design and performance evaluation is shown in Table 1. The following outlines the main findings of these studies:

- Optimum ejector operation occurs at the critical condition. The condenser pressure controls the location of the shock wave, where an increase in the condenser pressure above the critical point results in a rapid decline of the ejector entrainment ratio, since the shock wave moves towards the nozzle exit. Operating at pressures below the critical points has negligible effect on the ejector entrainment ratio.
- At the critical condition, the ejector entrainment ratio increases at lower pressure for the boiler and condenser. Also, higher temperature for the evaporator increases the entrainment ratio.
- Use of a variable position nozzle can maintain the optimum conditions for ejector operation. As a result, the ejector can be maintained at critical conditions even if the operating conditions are varied.
- Multi-ejector system increases the operating range and improves the overall system efficiency.
- Ejector modeling is essential for better understanding of the compression process, system design and performance evaluation. Models include empirical correlations, such as those by Ludwig [1], Power [2] and El-Dessouky and Ettouney [3]. Such models are limited to the range over which it was developed, which limits their use in investigating the performance of new ejector fluids, designs or operating conditions. Semi-empirical models give more flexibility in ejector design and performance evaluation [4,5]. Other ejector models are based on fundamental balance equations [6].

This study is motivated by the need for a simple empirical model that can be used to design and evaluate the performance of steam jet ejectors. The model is based on a large database extracted from several ejector manufacturers and a number of experimental literature studies. As will be discussed later, the model is simple to use and it eliminates the need for iterative procedures.

2. Mathematical model

The review by Sun and Eames [7] outlined the developments in mathematical modeling and design of jet ejectors. The review shows that there are two basic approaches for ejector analysis. These include mixing of the motive steam and entrained vapor, either at constant pressure or at constant area. Design models of stream mixing at constant pressure are more common in literature because the performance of the ejectors designed by this method is more superior to the constant area method and it compares favorably against experimental data. The basis for modeling the constant pressure design procedure was initially developed by Keenan [6]. Subsequently, several investigators have used the model for design and performance evaluation of various types of jet ejectors. This involved a number of modifications in the model, especially losses within the ejector and mixing of the primary and secondary streams. In this section, the constant pressure ejector model is developed. The developed model is based on a number of literature studies [8–11].

The constant pressure model is based on the following assumptions:

Table 1
Summary of literature studies on ejector design and performance

Reference	Fluid	Boiler, evaporator and condenser temperature (°C)	Conclusion
[19]	R-113	60–100; 5–18; 40–50	Basis for refrigerant selection for solar system, system performance increased with increasing boiler and evaporator temperatures and decreasing condenser temperature.
[20]	R-113; R-114; R-142b; R-718	80–95; 5–13; 25–45	Comparison of ejector and refrigerant performance. Dry, wet and isentropic fluids. Wet fluid damage ejectors due phase change during isentropic expansion. R-113 (dry) has the best performance and R142b (wet) has the poorest performance.
[21,22]	R-114	86; −8; 30	Increase in ejector performance using mechanical compression booster.
[8]	Water	120–140; 5–10; 30–65	Choking of the entrained fluid in the mixing chamber affects system performance. Maximum COP is obtained at the critical flow condition.
[13]	Water	120–140; 5–10; 30–60	Effect of varying the nozzle position to meet operating condition. Increase in COP and cooling capacity by 100%.
[23]	R-113	70–100; 6–25; 42–50	Entrainment ratio is highly affected by the condenser temperature especially at low evaporator temperature.
[24]	R-11	82.2–182.2; 10; 43.3	Entrainment ratio is proportional to boiler temperature.
[25,26]	R-114	90; 4; 30	Combined solar generator and ejector air conditioner. More efficient system requires multi-ejector and cold energy storage (cold storage in either phase changing materials, cold water or ice).
[27]	R-134A	−15; 30	Modeling the effect of motive nozzle on system performance, in which the ejector is used to recover part of the work that would be lost in the expansion valve using high-pressure motive liquid.
[28]	Water	100–165; 10; 30–45	Combined solar collector, refrigeration and seawater desalination system. Performance depends on steam pressure, cooling water temperature and suction pressure.
[4]	Water		Developed a new ejector theory in which the entrained fluid is choked, the plant scale results agree with this theory. Steam jet refrigeration should be designed for the most often prevailing conditions rather than the most severe to achieve greater overall efficiency.
[29]	Water	–	Model of multistage steam ejector refrigeration system using annular ejector in which the primary fluid enters the second stage at annular nozzle on the sidewall. This will increase static pressure for low-pressure stream and mixture and reduce the velocity of the motive stream and reduce jet mixing losses shock wave formation losses.
[24]	R11; R113; R114	93.3; 10; 43.3	Measure and calculate ejector entrainment ratio as a function of boiler, condenser and evaporator temperatures. Entrainment ratio decreases for off design operation and increases for the two stage ejectors.
[30]	R113; R114; R142b	120–140; 65–80	Effect of throat area, location of main nozzle and length of the constant area section on backpressure, entrainment ratio and compression ratio.
[5]			Mathematical model use empirical parameters that depend solely on geometry. The parameters are obtained experimentally for various types of ejectors.
[31]	R134a	5; −12, −18; 40	Combined ejector and mechanical compressor for operation of domestic refrigerator-freezer increases entrainment ratio from 7 to 12.4%. The optimum throat diameter depends on the freezer temperature
[9]	R11; HR-123	80; 5; 30	Performance of HR-123 is similar to R-11 in ejector refrigeration. Optimum performance is achieved by the use of variable geometry ejector when operation conditions change.

1. The motive steam expands isentropically in the nozzle. Also, the mixture of the motive steam and the entrained vapor compresses isentropically in the diffuser.
2. The motive steam and the entrained vapor are saturated and their velocities are negligible.
3. Velocity of the compressed mixture leaving the ejector is insignificant.
4. Constant isentropic expansion exponent and the ideal gas behavior.
5. The mixing of motive steam and the entrained vapor takes place in the suction chamber.
6. The flow is adiabatic.
7. Friction losses are defined in terms of the isentropic efficiencies in the nozzle, diffuser and mixing chamber.
8. The motive steam and the entrained vapor have the same molecular weight and specific heat ratio.
9. The ejector flow is one-dimensional and at steady state conditions.

The model equations include the following:

- Overall material balance

$$m_p + m_e = m_c \tag{1}$$

where m is the mass flow rate and the subscripts c, e and p, define the compressed vapor mixture, the entrained vapor and the motive steam or primary stream.

- Entrainment ratio

$$w = m_e/m_p \tag{2}$$

- Compression ratio

$$\mathrm{Cr} = P_c/P_e \tag{3}$$

- Expansion ratio

$$\mathrm{Er} = P_p/P_e \tag{4}$$

- Isentropic expansion of the primary fluid in the nozzle is expressed in terms of the Mach number of the primary fluid at the nozzle outlet plane

$$M_{p_2} = \sqrt{\frac{2\eta_n}{\gamma - 1}\left[\left(\frac{P_p}{P_2}\right)^{(\gamma-1/\gamma)} - 1\right]} \tag{5}$$

where M is the Mach number, P is the pressure and γ is the isentropic expansion coefficient. In the above equation, η_n is the nozzle efficiency and is defined as the ratio between the actual enthalpy change and the enthalpy change undergone during an isentropic process.

- Isentropic expansion of the entrained fluid in the suction chamber is expressed in terms of the Mach number of the entrained fluid at the nozzle exit plane

$$M_{e_2} = \sqrt{\frac{2}{\gamma - 1}\left[\left(\frac{P_e}{P_2}\right)^{(\gamma-1/\gamma)} - 1\right]} \tag{6}$$

- The mixing process is modeled by one-dimensional continuity, momentum and energy equations. These equations are combined to define the critical Mach number of the mixture at point 5 in terms of the critical Mach number for the primary and entrained fluids at point 2

$$M_4^* = \frac{M_{p_2}^* + wM_{e_2}^*\sqrt{T_e/T_p}}{\sqrt{(1+w)(1+wT_e/T_p)}} \tag{7}$$

where w is the entrainment ratio and M^* is the ratio between the local fluid velocity to the velocity of sound at critical conditions.

- The relationship between M and M^* at any point in the ejector is given by this equation

$$M^* = \sqrt{\frac{M^2(\gamma+1)}{M^2(\gamma-1)+2}} \tag{8}$$

Eq. (8) is used to calculate $M_{e_2}^*$, $M_{p_2}^*$, M_4

- Mach number of the mixed flow after the shock wave

$$M_5 = \frac{M_4^2 + \dfrac{2}{(\gamma-1)}}{\dfrac{2\gamma}{(\gamma-1)}M_4^2 - 1} \tag{9}$$

- Pressure increase across the shock wave at point 4

$$\frac{P_5}{P_4} = \frac{1+\gamma M_4^2}{1+\gamma M_5^2} \tag{10}$$

In Eq. (10) the constant pressure assumption implies that the pressure between points 2 and 4 remains constant. Therefore, the following equality constraint applies $P_2 = P_3 = P_4$.

- Pressure lift in the diffuser

$$\frac{P_c}{P_5} = \left[\frac{\eta_d(\gamma-1)}{2}M_5^2 + 1\right]^{(\gamma/\gamma-1)} \tag{11}$$

where η_d is the diffuser efficiency.

- The area of the nozzle throat

$$A_1 = \frac{m_p}{P_p}\sqrt{\frac{RT_p}{\gamma\eta_n}\left(\frac{\gamma+1}{2}\right)^{(\gamma+1)/(\gamma-1)}} \tag{12}$$

- The area ratio of the nozzle throat and diffuser constant area

$$\frac{A_1}{A_3} = \frac{P_c}{P_p}\left(\frac{1}{(1+w)(1+w(T_e/T_p))}\right)^{1/2} \frac{\left(\dfrac{P_2}{P_c}\right)^{1/\gamma}\left(1-\left(\dfrac{P_2}{P_c}\right)^{(\gamma-1)/\gamma}\right)^{1/2}}{\left(\dfrac{2}{\gamma+1}\right)^{1/(\gamma-1)}\left(1-\dfrac{2}{\gamma+1}\right)^{1/2}} \tag{13}$$

- The area ratio of the nozzle throat and the nozzle outlet

$$\frac{A_2}{A_1}=\sqrt{\frac{1}{M_{p_2}^2}\left(\frac{2}{(\gamma+1}\left(1+\frac{(\gamma-1)}{2}M_{p_2}^2\right)\right)^{(\gamma+1)/(\gamma-1)}} \quad (14)$$

3. Solution procedure

Two solution procedures for the above model are shown in Fig. 2. Either procedure requires iterative calculations. The first procedure is used for system design, where the system pressures and the entrainment ratio is defined. Iterations are made to determine the pressure of the motive steam at the nozzle outlet (P_2) that gives the same back pressure (P_c). The iteration sequence for this procedure is shown in Fig. 2(a) and it includes the following steps:

- Define the design parameters, which include the entrainment ratio (w), the flow rate of the compressed vapor (m_c) and the pressures of the entrained vapor, compressed vapor and motive steam (P_e, P_p, P_c).
- Define the efficiencies of the nozzle and diffuser (η_n, η_d).
- Calculate the saturation temperatures for the compressed vapor, entrained vapor and motive steam, which include T_c, T_p, T_e, using the saturation temperature correlation given in the appendix.
- As for the universal gas constant and the specific heat ratio for steam, their values are taken as 0.462 and 1.3.
- The flow rates of the entrained vapor (m_e) and motive steam (m_p) are calculated from Eqs. (1) and (2).
- A value for the pressure at point 2 (P_2) is estimated and Eqs. (5)–(11) are solved sequentially to obtain the pressure of the compressed vapor (P_c).
- The calculated pressure of the compressed vapor is compared to the design value.
- A new value for P_2 is estimated and the previous step is repeated until the desired value for the pressure of the compressed vapor is reached.

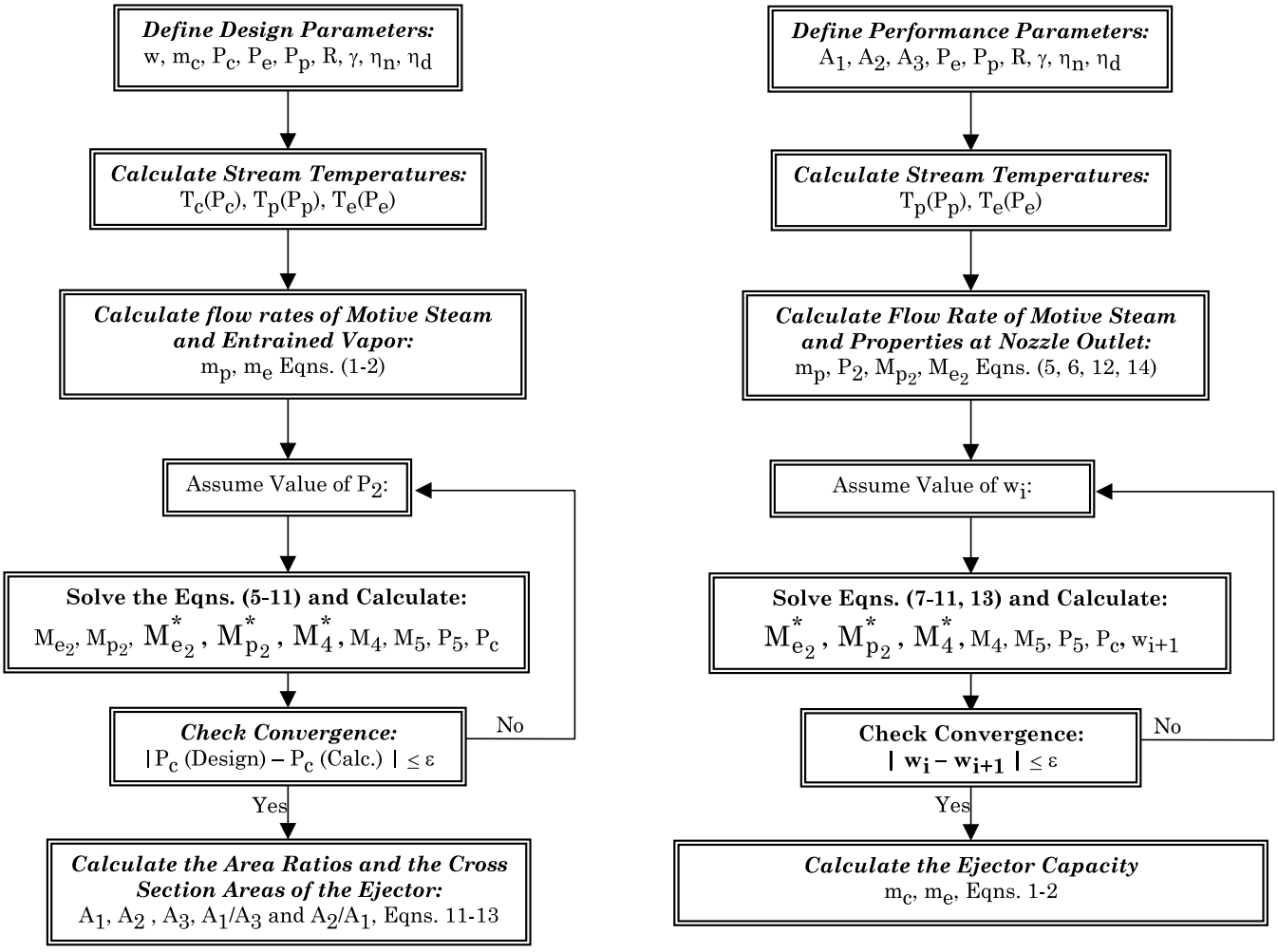

Fig. 2. Solution algorithms of the mathematical model. (a) Design procedure to calculate area ratios. (b) Performance evaluation to calculate w.

- The ejector cross section areas (A_1, A_2, A_3) and the area ratios (A_1/A_3 and A_2/A_1) are calculated from Eqs. (12)–(14).

The second solution procedure is used for performance evaluation, where the cross section areas and the entrainment and motive steam pressures are defined. Iterations are made to determine the entrainment ratio that defines the ejector capacity. The iteration sequence for this procedure is shown in Fig. 2(b) and it includes the following steps:

- Define the performance parameters, which include the cross section areas (A_1, A_2, A_3), the pressures of the entrained vapor (P_e) and the pressure of the primary stream (P_p).
- Define the efficiencies of the nozzle and diffuser (η_n, η_d).
- Calculate the saturation temperatures of the primary and entrained streams, T_p and T_e, using the saturation temperature correlation given in the appendix.
- As for the universal gas constant and the specific heat ratio for steam, their values are taken as 0.462 and 1.3.
- Calculate the flow rate of the motive steam and the properties at the nozzle outlet, which include m_p, P_2, M_{e2}, M_{p2}. These are obtained by solving Eqs. (5), (6), (12) and (14).
- An estimate is made for the entrainment ratio, w.
- This value is used to calculate other system parameters defined in Eqs. (7)–(11), which includes $M^*_{e_2}$, $M^*_{p_2}$, M^*_4, M_4, M_5, P_5, P_c.
- A new estimate for w is obtained from Eq. (13).
- The error in w is determined and a new iteration is made if necessary.
- The flow rates of the compressed and entrained vapor are calculated from Eqs. (1) and (2).

4. Semi-empirical model

Development of the semi-empirical model is thought to provide a simple method for designing or rating of steam jet ejectors. As shown above, solution of the mathematical model requires an iterative procedure. Also, it is necessary to define values of η_n and η_d. The values of these efficiencies widely differ from one study to another, as shown in Table 2. The semi-empirical model for the steam jet ejector is developed over a wide range of operating conditions. This is achieved by using three sets of design data acquired from major ejector manufacturers, which includes Croll Reynolds, Graham and Schutte–Koerting. Also, several sets of experimental data are extracted from the literature and are used in the development of the empirical model. The semi-empirical model includes a number of correlations to calculate the entrainment ratio (w), the pressure at the nozzle outlet (P_2) and the area ratios in the ejector (A_2/A_1) and (A_1/A_3). The correlation for the entrainment ratio is developed as a function of the expansion ratio and the pressures of the motive steam, the entrained vapor and the compressed vapor. The correlation for the pressure at the nozzle outlet is developed as a function of the evaporator and condenser pressures. The correlations for the ejector area ratios are defined in terms of the system pressures and the entrainment ratio. Table 3 shows a summary of the ranges of the experimental and the design data. The table also includes the ranges for the data reported by Power [12].

Table 2
Examples of ejector efficiencies used in literature studies

Reference	η_n	η_d	η_m
[27]	0.9	0.75	
[32]		0.8	0.8
[33]	0.85	0.85	
[31]	0.7–1	0.7–1	
[10]	0.8–1	0.8–1	
[24]	0.85–0.98	0.65–0.85	
[8]	0.85	0.85	0.95
[34]	0.75	0.9	

A summary of the experimental data, which is used to develop the semi-empirical model is shown in Table 4. The data includes measurements by the following investigators:

- Eames et al. [8] obtained the data for a compression ratio of 3–6, expansion ratio 160–415 and entrainment ratio of 0.17–0.58. The measurements are obtained for an area ratio of 90 for the diffuser and the nozzle throat.
- Munday and Bagster [4] obtained the data for a compression ratio of 1.8–2, expansion ratio of 356–522 and entrainment ratio of 0.57–0.905. The measurements are obtained for an area ratio of 200 for the diffuser and the nozzle throat.
- Aphornratana and Eames [13] obtained the data for a compression ratio of 4.6–5.3, expansion ratio of 309.4 and entrainment ratio of 0.11–0.22. The measurements are obtained for an area ratio of 81 for the diffuser and the nozzle throat.
- Bagster and Bresnahan [14] obtained the data for a compression ratio of 2.4–3.4, expansion ratio of 165–426 and entrainment ratio of 0.268–0.42. The measurements are obtained for an area ratio of 145 for the diffuser and the nozzle throat.
- Sun [15] obtained the data for a compression ratio of 2.06–3.86, expansion ratio of 116–220 and entrainment ratio of 0.28–0.59. The measurements are obtained for an area ratio of 81 for the diffuser and the nozzle throat.
- Chen and Sun [16] obtained the data for a compression ratio of 1.77–2.76, expansion ratio of 1.7–2.9 and entrainment ratio of 0.37–0.62. The measure-

ments are obtained for an area ratio of 79.21 for the diffuser and the nozzle throat.

- Arnold et al. [17] obtained the data for a compression ratio of 2.47–3.86, expansion ratio of 29.7–46.5, and entrainment ratio of 0.27–0.5.
- Everitt and Riffat [18] obtained the data for a compression ratio of 1.37–2.3, expansion ratio of 22.6–56.9 and entrainment ratio of 0.57.

The correlation for the entrainment ratio of choked flow or compression ratios above 1.8 is given by

$$W = aEr^{b}P_{e}^{c}P_{c}^{d}\frac{(e+fP_{p}^{g})}{(h+iP_{c}^{j})} \quad (15)$$

Similarly, the correlation for the entrainment ratio of un-choked flow with compression ratios below 1.8 is given by

$$W = aEr^{b}P_{e}^{c}P_{c}^{d}\frac{(e+f\ln(P_{p}))}{(g+h\ \ln(P_{c}))} \quad (16)$$

The constants in Eqs. (15) and (16) are given as follows

	Entrainment ratio correlation choked flow (Eq. (15); Fig. 3)	Entrainment ratio correlation non-choked flow (Eq. (16), Fig. 4)
a	0.65	-1.89×10^{-5}
b	−1.54	−5.32
c	1.72	5.04
d	6.79v10^{-2}	9.05×10^{-2}
e	22.82	22.09
f	4.21×10^{-4}	−6.13
g	1.34	0.82
h	9.32	-3.37×10^{-5}
j	1.28×10^{-1}	–
j	1.14	–
R^2	0.85	0.79

Fitting results against the design and experimental data are shown in Figs. 3 and 4, respectively. The results shown in Fig. 3 cover the most commonly used range for steam jet ejectors, especially in vacuum and vapor compression applications. As shown in Fig. 3, the fitting result is very satisfactory for entrainment ratios between 0.2 and 1. This is because the major part of the data is found between entrainment ratios clustered over a range of 0.2–0.8. Examining the experimental data fit shows that the major part of the data fit is well within the correlation predictions, except for a small number of points, where the predictions have large deviations.

The correlations for the motive steam pressure at the nozzle outlet and the area ratios are obtained semi-empirically. In this regard, the design and experimental data for the entrainment ratio and system pressures are used to solve the mathematical model and to calculate the area ratios and motive steam pressure at the nozzle outlet. The results are obtained for efficiencies of 100% for the diffuser, nozzle and mixing and a value of 1.3 for γ. The results are then correlated as a function of the system variables. The following relations give the correlations for the choked flow:

$$P_2 = 0.13\ P_{e}^{0.33}P_{c}^{0.73} \quad (17)$$

$$A_1/A_3 = 0.34\ P_{c}^{1.09}P_{p}^{-1.12}w^{-0.16} \quad (18)$$

$$A_2/A_1 = 1.04\ P_{c}^{-0.83}P_{p}^{0.86}w^{-0.12} \quad (19)$$

The R^2 for each of the above correlations is above 0.99. Similarly, the following relations give the correlations for the un-choked flow:

$$P_2 = 1.02\ P_{e}^{-0.000762}P_{c}^{0.99} \quad (20)$$

$$A_1/A_3 = 0.32\ P_{c}^{1.11}P_{p}^{-1.13}w^{-0.36} \quad (21)$$

$$A_2/A_1 = 1.22\ P_{c}^{-0.81}P_{p}^{0.81}w^{-0.0739} \quad (22)$$

The R^2 values for the above three correlations are above 0.99.

The semi-empirical ejector design procedure involves sequential solution of Eqs. (1)–(14) together with Eq. (17) or Eq. (20) (depending on the flow type, choked or non-choked). This procedure is not iterative in contrast with the procedure given for the mathematical model in the previous section. As for the semi-empirical performance evaluation model, it involves non-iterative solution of Eqs. (1)–(14) together with Eq. (15) or Eq. (16) for choked or non-choked flow, respectively. It should be stressed that both solution procedures are indepen-

Table 3
Range of design and experimental data used in model development

Source	Er	Cr	P_e (kPa)	P_c (kPa)	P_p (kPa)	w
Experimental	1.4–6.19	1.6–526.1	0.872–121.3	2.3–224.1	38.6–1720	0.11–1.132
Schutte–Koerting	1.008–3.73	1.36–32.45	66.85–2100.8	790.8–2859.22	84.09–2132.27	0.1–4
Croll–Rynolds	1.25–4.24	4.3–429.4	3.447–124.1	446.06–1480.27	6.2–248.2	0.1818–2.5
Graham	1.174–4.04	4.644–53.7	27.58–170.27	790.8–1480.27	34.47–301.27	0.18–3.23
Power	1.047–5.018	2–1000	2.76–172.37	3.72–510.2	344.74–2757.9	0.2–4

Table 4
Summary of literature experimental data for steam jet ejectors

A_d/A_t	P_p (kPa)	P_e (kPa)	P_c (kPa)	P_p/P_e	P_c/P_e	w	Reference
90	198.7	1.23	3.8	161.8	3.09	0.59	[8]
	232.3	1.23	4.2	189.1	3.42	0.54	[8]
	270.3	1.23	4.7	220.1	3.83	0.47	[8]
	313.3	1.23	5.3	255.1	4.31	0.39	[8]
	361.6	1.23	6	294.4	4.89	0.31	[8]
90	198.7	1.04	3.6	191.6	3.47	0.5	[8]
	232.3	1.04	4.1	223.9	3.95	0.42	[8]
	270.3	1.04	4.6	260.7	4.44	0.36	[8]
	313.3	1.04	5.1	302.1	4.91	0.29	[8]
	361.6	1.04	5.7	348.7	5.49	0.23	[8]
90	198.7	0.87	3.4	227.7	3.89	0.4	[8]
	232.3	0.87	3.7	266.2	4.24	0.34	[8]
	270.3	0.87	4.4	309.8	5.04	0.28	[8]
	313.3	0.87	5.1	359	5.85	0.25	[8]
	361.6	0.87	5.4	414.4	6.19	0.18	[8]
200	834	1.59	3.2	521.7	2.0	0.58	[4]
	400	1.59	3.07	250.2	1.92	1.13	[4]
	669	1.71	3.67	392.3	2.15	0.58	[4]
	841	1.59	3.51	526.1	2.19	0.51	[4]
	690	1.94	3.38	356	1.74	0.86	[4]
	690	1.94	3.51	356	1.81	0.91	[4]
81	270	0.87	4.1	309.5	4.7	0.22	[13]
	270	0.87	4.2	309.5	4.8	0.19	[13]
	270	0.87	4.4	309.5	5.04	0.16	[13]
	270	0.87	4.5	309.5	5.16	0.14	[13]
	270	0.87	4.7	309.5	5.39	0.11	[13]
145	660	1.55	5.3	426.5	3.42	0.27	[14]
	578	1.55	5.3	373.5	3.42	0.31	[14]
	516	1.58	5.3	326.9	3.36	0.35	[14]
	440	1.57	5.03	280.6	3.21	0.38	[14]
	381	1.59	4.77	239.9	3	0.42	[14]
	312	1.62	4.23	192.6	2.61	0.46	[14]
	278	1.68	4.1	165.1	2.44	0.42	[14]
81	143.4	1.23	2.53	116.8	2.06	0.59	[15]
	169.2	1.23	2.67	137.8	2.17	0.51	[15]
	198.7	1.23	3.15	161.8	2.56	0.43	[15]
	232.3	1.23	4	189.1	3.26	0.35	[15]
	270.3	1.23	4.75	220.1	3.87	0.29	[15]
	1720	57.7	143	29.7	2.47	0.5	[17]
	1720	51.4	143	33.5	2.78	0.4	[17]
	1720	45.5	143	37.8	3.14	0.3	[17]
	1720	37.01	143	46.5	3.86	0.27	[17]
79.21	116	67.6	119.9	1.7	1.8	0.62	[16]
	153	67.6	151.7	2.3	2.2	0.49	[16]
	270	67.6	224.1	3.9	3.3	0.34	[16]
	198	121.3	195.1	1.6	1.6	0.78	[16]
	198	99.9	195.1	1.9	1.9	0.64	[16]
	198	67.6	186.2	2.9	2.8	0.37	[16]
	57.9	1.02	2.3	56.9	2.3	0.57	[18]
	47.4	1.2	2.3	38.6	1.9	0.56	[18]
	38.6	1.7	2.3	22.6	1.4	0.57	[18]

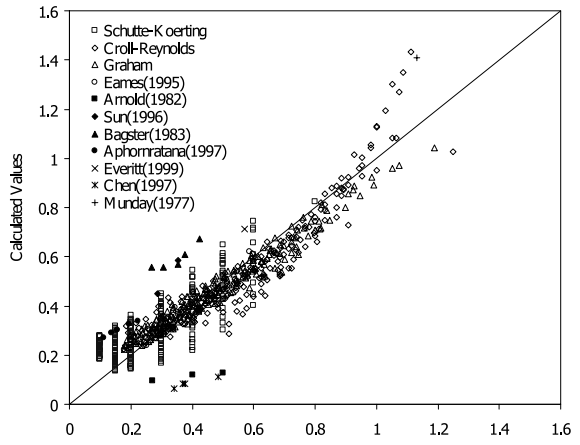

Fig. 3. Fitting of the entrainment ratio for compression ratios higher than 1.8.

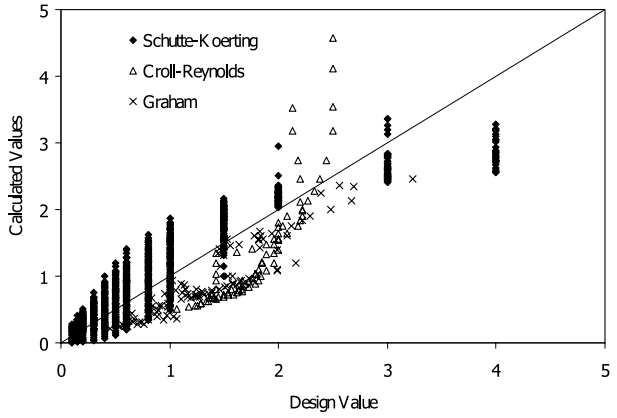

Fig. 4. Fitting of the entrainment ratio for compression ratios lower than 1.8.

dent of the nozzle and diffuser efficiencies, which varies over a wide range, as shown in Table 2.

5. Conclusions

A semi-empirical model is developed for design and performance evaluation of steam jet ejector. The model includes correlations for the entrainment ratio in choked and non-choked flow, the motive steam pressure at the nozzle outlet and the area ratios of the ejector. The correlations for the entrainment ratio are obtained by fitting against a large set of design data and experimental measurements. In addition, the correlations for the motive steam pressure at the nozzle outlet and the area ratios are obtained semi-empirically by solving the mathematical model using the design and experimental data for the entrainment ratio and system pressures. The correlations cover a wide range of compression, expansion and entrainment ratios, especially those used in industrial applications. The developed correlations are simple and very useful for design and rating calculations, since it can be used to determine the entrainment ratio, which, upon specification of the system load, can be used to determine the motive steam flow rate and the cross section areas of the ejector.

Acknowledgements

The authors would like to acknowledge funding support of the Kuwait University Research Administration, Project No. EC084 entitled 'Multiple Effect Evaporation and Absorption/Adsorption Heat Pumps'.

Appendix A. Nomenclature

A	cross section area (m^2)
COP	coefficient of performance, dimensionless
Cr	compression ratio defined as pressure of compressed vapor to pressure of entrained vapor
Er	expansion ratio defined as pressure of compressed vapor to pressure of entrained vapor
m	mass flow rate (kg/s)
M	Mach number, ratio of fluid velocity to speed of sound
M^*	critical Mach number, ratio of fluid velocity to speed of sound
P	pressure (kPa)
ΔP	pressure drop (kPa)
R	universal gas constant (kJ/kg °C)
Rs	load ratio, mass flow rate of motive steam to mass flow rate of entrained vapor
T	temperature (K)
w	entrainment ratio, mass flow rate of entrained vapor to mass flow rate of motive steam

Greek symbols

γ	compressibility ratio
η	ejector efficiency

Subscripts

1–7	locations inside the ejector
b	boiler
c	condenser
d	diffuser
e	evaporator or entrained vapor
m	mixing
n	nozzle
p	primary stream or motive steam
t	throat of the nozzle

Appendix B

B.1. Correlations of saturation pressure and temperature

The saturation temperature correlation is given by

$$T = \left(42.6776 - \frac{3892.7}{(\ln(P/1000) - 9.48654)}\right) - 273.15$$

where P is in kPa and T is in °C. The above correlation is valid for the calculated saturation temperature over a pressure range of 10–1750 kPa. The percentage errors for the calculated versus the steam table values are $< 0.1\%$.

The correlation for the water vapor saturation pressure is given by

$$\ln(P/P_c) = \left(\frac{T_c}{T + 273.15} - 1\right) \times \sum_{i=1}^{8} f_i (0.01(T + 273.15 - 338.15))^{(i-1)}$$

where $T_c = 647.286$ K and $P_c = 22089$ kPa and the values of f_i are given in the following table

f_1	f_2	f_3	f_4
−7.419242	0.29721	−0.1155286	0.008685635
f_5	f_6	f_7	f_8
0.001094098	−0.00439993	0.002520658	−0.000521868

where P and T are in kPa and °C. The above correlation is valid over a temperature range of 5–200 °C with a percentage error of $< 0.05\%$ for the corresponding values in the steam tables.

References

[1] E.E. Ludwig, Applied Process Design for Chemical and Petrochemical Plants, vol. 1, second ed, Gulf, Houston, TX, 1977.
[2] R.B. Power, Hydrocarb. Proc. 43 (1964) 138.
[3] H.T. El-Dessouky, H.M. Ettouney, Single effect thermal vapor compression desalination process: thermal analysis, Heat Trans. Eng. 20 (1999) 52–68.
[4] J.T. Munday, D.F. Bagster, A new ejector theory to steam jet refrigeration, IEC 16 (1977) 442–449.
[5] H.J. Henzler, Design of ejectors for single-phase material systems, Ger. Chem. Eng. 6 (1983) 292–300.
[6] J.H. Keenan, E.P. Neumann, A simple air ejector, J. Appl. Mech. 64 (1942) 85–91.
[7] D.W. Sun, I.W. Eames, Recent developments in the design theories and applications of ejectors—a review, J. Inst. Energy 68 (1995) 65–79.
[8] I.W. Eames, S. Aphornaratana, H. Haider, A theoretical and experimental study of a small-scale steam jet refrigerator, Int. J. Refrig. 18 (1995) 378–385.
[9] D.W. Sun, I.W. Eames, Performance characteristics of HCFC-123 ejector refrigeration cycle, Int. J. Energy Res. 20 (1996) 871–885.
[10] N.H. Aly, A. Karmeldin, M.M. Shamloul, Modelling and simulation of steam jet ejectors, Desalination 123 (1999) 1–8.
[11] B.J. Huang, J.M. Chang, C.P. Wang, V.A. Petrenko, A 1-D analysis of ejector performance, Int. J. Refrig. 22 (1999) 354–364.
[12] R.B. Power, Predicting unstable-mode performance of a steam jet ejector, Am. Soc. Mech. Eng. FSPI 1 (1994) 11–15.
[13] S. Aphornratana, I.W. Eames, A small capacity steam-ejector refrigerator: experimental investigation of a system using ejector with moveable primary nozzle, Int. J. Refrig. 20 (1997) 352–358.
[14] D.F. Bagster, J.D. Bresnahan, An examination of the two-stream theory of steam-jet ejectors, Proceedings of the Eleventh Australian Conference on Chemical Engineering, Brisbane, 4–7 September, 1983.
[15] D. Sun, Variable geometry ejectors and their applications in ejector refrigeration systems, Energy 21 (1996) 919–929.
[16] Y.M. Chen, C.Y. Sun, Experimental study of the performance characteristics of a steam-ejector refrigeration system, Exper. Therm. Fluid Sci. 15 (1997) 384–394.
[17] H.G. Arnold, W.R. Huntley, H. Perez-Blanco, Steam ejector as an industrial heat pump, ASHRAE Trans. 88 (1982) 845–857.
[18] P. Everitt, S.B. Riffat, Steam jet ejector system for vehicle air conditioning, Int. J. Amb. Energy 20 (1999) 14–20.
[19] N. Al-Khalidy, Performance of solar refrigerant ejector refrigerating machine, ASHRAE Trans. 103 (1997) 56–64.
[20] S.L. Chen, J.Y. Yen, M.C. Huang, An experimental investigation of ejector performance based upon different refrigerants, ASHRAE Trans. 104 (1998) 153–160.
[21] M. Sokolov, D. Hershgal, Enhanced ejector refrigeration cycles powered by low grade heat. Part 1. Systems characterization, Int. J. Refrig. 13 (1990a) 351–356.
[22] M. Sokolov, D. Hershgal, Enhanced ejector refrigeration cycles powered by low grade heat. Part 2. Design procedures, Int. J. Refrig. 13 (1990b) 357–363.
[23] N. Al-Khalidy, A. Zayonia, Design and experimental investigation of an ejector in an air-conditioning and refrigeration system, ASHRAE Trans. 101 (1995) 383–391.
[24] F.C. Chen, C.T. Hsu, Performance of ejector heat pumps, Energy Res. 11 (1987) 289–300.
[25] M. Sokolov, D. Hershgal, Optimal coupling and feasibility of solar powered year-round ejector air conditioner, Sol. Energy 50 (1993a) 507–516.
[26] M. Sokolov, D. Hershgal, Solar-powered compression-enhanced ejector air conditioner, Sol. Energy 51 (1993b) 183–194.
[27] P. Menegay, A.A. Kornhauser, Ejector expansion refrigeration cycle with underexpanded motive nozzle, Am. Inst. Aeronaut. Astronaut. 2 (1994) 915–920.
[28] H.K. Abdel-Aal, A.S. Al-Zakri, M.E. El-Sarha, M.E. El-Swify, G.M. Assassa, Other options of mass and energy input for steam jet refrigeration systems, Chem. Eng. J. 45 (1990) 99–110.
[29] G. Grazzini, A. Mariani, A simple program to design a multi-stage jet-pump for refrigeration cycles, Energy Convers. Manag. 39 (1998) 1827–1834.
[30] M.C. Huang, S.L. Chen, An experimental investigation of ejector performance characteristics in a jet refrigeration system, J. Chin. Inst. Chem. Eng. 27 (1996) 91–100.
[31] M.L. Tomasek, R. Radermacher, Analysis of a domestic refrigerator cycle with an ejector, ASHRAE Trans. 1 (1995) 1431–1438.
[32] E.D. Rogdakis, G.K. Alexis, Design and parametric investigation of an ejector in an air-conditioning system, Appl. Therm. Eng. 20 (2000) 213–226.
[33] D.W. Sun, Comparative study of the performance of an ejector refrigeration cycle operating with various refrigerants, Energy Convers. Manag. 40 (1999) 873–884.
[34] S.K. Gupta, R.P. Singh, R.S. Dixit, A comparative parametric study of two theoretical models of a single-stage single-fluid, steam jet ejector, Chem. Eng. J. 18 (1979) 81–85.